HEALTH AND MEDICINE

An innovative biologic system for photon-powered myocardium in the ischemic heart

Jeffrey E. Cohen,[1] Andrew B. Goldstone,[1] Michael J. Paulsen,[1] Yasuhiro Shudo,[1] Amanda N. Steele,[1] Bryan B. Edwards,[1] Jay B. Patel,[1] John W. MacArthur Jr.,[1] Michael S. Hopkins,[1] Casey E. Burnett,[2] Kevin J. Jaatinen,[1] Akshara D. Thakore,[1] Justin M. Farry,[1] Vi N. Truong,[1] Alexandra T. Bourdillon,[1] Lyndsay M. Stapleton,[1] Anahita Eskandari,[1] Alexander S. Fairman,[3] William Hiesinger,[1] Tatiana V. Esipova,[3] William L. Patrick,[1] Keven Ji,[3] Judith A. Shizuru,[2] Y. Joseph Woo[1]*

Coronary artery disease is one of the most common causes of death and disability, afflicting more than 15 million Americans. Although pharmacological advances and revascularization techniques have decreased mortality, many survivors will eventually succumb to heart failure secondary to the residual microvascular perfusion deficit that remains after revascularization. We present a novel system that rescues the myocardium from acute ischemia, using photosynthesis through intramyocardial delivery of the cyanobacterium *Synechococcus elongatus*. By using light rather than blood flow as a source of energy, photosynthetic therapy increases tissue oxygenation, maintains myocardial metabolism, and yields durable improvements in cardiac function during and after induction of ischemia. By circumventing blood flow entirely to provide tissue with oxygen and nutrients, this system has the potential to create a paradigm shift in the way ischemic heart disease is treated.

INTRODUCTION

Cardiovascular disease is the leading cause of death globally and accounts for nearly $1 trillion in costs annually (*1*). Over the past several decades, research and innovation have enabled advances in preventive, pharmacologic, and surgical strategies to greatly augment the clinician's ability to treat once devastating cardiac events. Stemming from these accomplishments, a wave of exploration into cardiac tissue regeneration (*2*, *3*) and angiogenesis (*4*, *5*) has yielded exciting results in preclinical models (*6*–*8*) and early clinical trials (*9*–*11*). Although these myocardial repair strategies have great popularity, development of alternative and uncharted pathways for the treatment of myocardial injury remains a critical need. Here, we report an innovative method for correcting myocardial ischemia by implementing a photosynthetic system where light, rather than blood, fuels cardiomyocytes.

Synechococcus elongatus is a naturally occurring unicellular cyanobacterium that photosynthesizes across a broad wavelength spectrum. It has traditionally been a research model for study of circadian rhythms (*12*, *13*) and, more recently, for enhanced production of biofuels using CO_2 as a carbon source. In addition, *S. elongatus* is easily engineered genetically to manipulate its metabolic activity for enhanced production of O_2 and glucose (*14*, *15*). On the basis of these characteristics, we hypothesized that *S. elongatus* could be used in vivo to clear CO_2 and provide ischemic cardiomyocytes with the essential O_2 and potentially also glucose, which are required for metabolic activity when blood flow is absent. In essence, *S. elongatus* might balance a traditionally unbalanced equation in an ischemic milieu involving CO_2, O_2, H_2O, and glucose. This allows light to become a fuel source for cardiomyocytes while potentially obviating the need for revascularization and restoration of perfusion.

Here, we demonstrate that delivery of *S. elongatus*, a photosynthetic cyanobacterium, to the ischemic heart greatly augments cardiac performance. Specifically, we found that cyanobacterial therapy increases tissue oxygenation, preserves myocardial metabolism, and enhances cardiac output (CO). Furthermore, this approach is nontoxic and does not elicit a meaningful immune response. These results represent an entirely novel strategy in leveraging photosynthesis to treat tissue ischemia, potentially forming the foundation of a new generation of medical therapeutics.

RESULTS

S. elongatus coexists with cardiomyocytes under mammalian physiological conditions in vitro and enhances cellular metabolism during hypoxia

Before investigating whether *S. elongatus* can provide therapeutic benefit to ischemic myocardium, we examined whether it tolerates physiological conditions found in mammals. After propagating a pure strain of *S. elongatus* and establishing a colony, we successfully cocultured the cyanobacteria with isolated rat cardiomyocytes (Fig. 1A). *S. elongatus* did not affect the survival of cardiomyocytes under standard conditions in vitro, as demonstrated by a live/dead cell viability assay performed on isolated neonatal rat cardiomyocytes cultured for 16 hours with and without *S. elongatus* (Fig. 1, B to D). We next evaluated whether *S. elongatus* can actively undergo photosynthesis under mammalian physiological conditions. Cardiomyocytes alone, *S. elongatus* at a concentration of 10^7 cells/ml, and cardiomyocytes with *S. elongatus* at a concentration of 10^7 cells/ml were cultured in Dulbecco's modified Eagle's medium with 10% fetal bovine serum (FBS) under both light and dark conditions (Fig. 1E). Cultures with *S. elongatus* demonstrated significantly higher oxygen levels under light than in dark condition, suggesting active photosynthesis. Cardiomyocytes cocultured with *S. elongatus* in the light trended toward higher oxygenation than did cardiomyocytes alone ($P = 0.1$). When compared to cultures containing *S. elongatus* alone, cardiomyocytes cocultured with *S. elongatus* exhibited significantly reduced oxygen levels under both light and dark conditions, suggesting that cardiomyocytes are consuming the excess oxygen.

Hypoxia was used to assess the ability of *S. elongatus* to enhance cellular metabolism in vitro. We performed a WST-1 cellular proliferation assay

[1]Department of Cardiothoracic Surgery, Stanford University School of Medicine, Stanford, CA 94305, USA. [2]Division of Blood and Marrow Transplantation, Department of Medicine, Stanford University School of Medicine, Stanford, CA 94305, USA. [3]Department of Biochemistry and Biophysics, Perelman School of Medicine, University of Pennsylvania, Philadelphia, PA 19104, USA.
*Corresponding author. Email: joswoo@stanford.edu

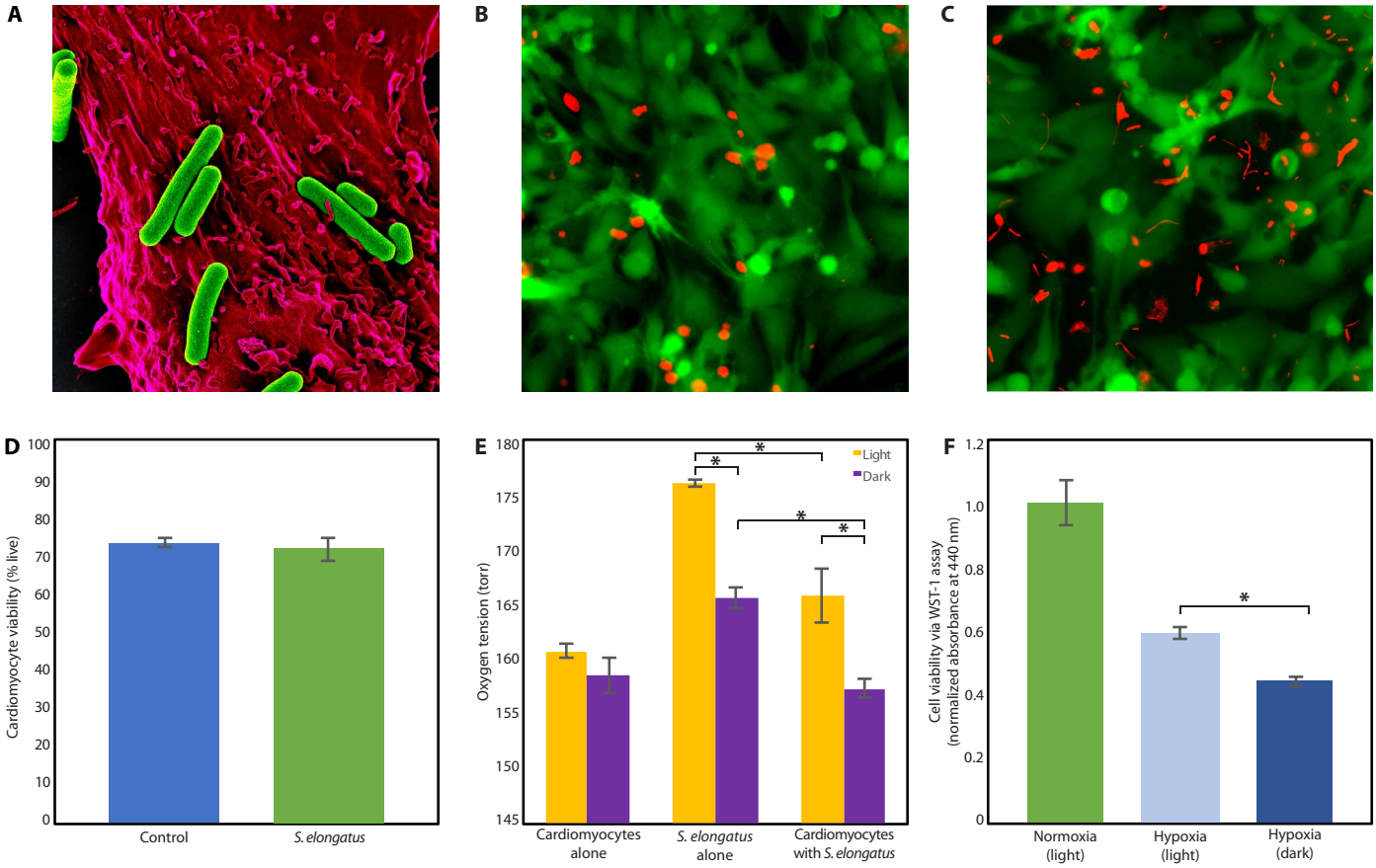

Fig. 1. *S. elongatus* successfully cocultured with rat cardiomyocytes. (**A**) False-colored scanning electron micrograph of multiple *S. elongatus* cyanobacteria (green) with a single rat cardiomyocyte (red). (**B** and **C**) Representative images of a live/dead assay of cardiomyocytes alone (B) and cardiomyocytes cocultured with *S. elongatus* (C). The cytoplasm of live cells is stained green, and the nuclei of dead cells are stained red; the autofluorescent rod-shaped *S. elongatus* are distinct from the circular dead nuclei. (**D**) Results of the live/dead assay demonstrating that the presence of *S. elongatus* does not affect cardiomyocyte survival. (**E**) In vitro oxygen measurements of cardiomyocytes alone, *S. elongatus* alone, and cardiomyocytes cocultured with *S. elongatus* under light and dark conditions in normoxia. In cultures containing *S. elongatus* alone and *S. elongatus* with cardiomyocytes, oxygen tension was significantly higher in the presence of light ($P < 0.01$ and $P = 0.03$, respectively), suggesting active photosynthesis. Cardiomyocytes cocultured with *S. elongatus* in the light demonstrated a positive trend toward increased oxygen when compared to cardiomyocytes alone ($P = 0.1$). When compared to cultures with *S. elongatus* alone, cultures with cardiomyocytes and *S. elongatus* demonstrated significantly reduced oxygen in light and dark ($P = 0.01$ and $P < 0.01$, respectively), suggesting oxygen consumption by cardiomyocytes. (**F**) Cellular viability was assessed using a WST-1 cell proliferation assay. Cardiomyocytes cultured with *S. elongatus* demonstrated significantly enhanced cellular metabolism in the presence of light as compared to dark ($P < 0.01$). All data are reported as means ± SEM. *$P < 0.05$ using two-tailed unpaired Student's *t* test.

on cardiomyocytes cocultured with 10^7 *S. elongatus* in normoxia, hypoxia with light, and hypoxia in darkness (Fig. 1F). The hypoxia-light group demonstrated a significant increase in cellular metabolism as compared to the hypoxia-dark group, suggesting that the oxygen generated by *S. elongatus* during photosynthesis may partially offset the cellular stress induced by hypoxia.

To determine whether increased glucose influenced the findings of enhanced metabolism, we investigated whether *S. elongatus* exports glucose. We measured glucose levels in a concentrated solution of 5×10^8 *S. elongatus* in 200 µl of BG-11 and compared this to the same volume of BG-11 alone under both light and dark conditions; glucose was undetectable in all samples.

Treatment of ischemic myocardium with *S. elongatus* significantly increases tissue oxygenation during acute myocardial infarction

To determine the effect of *S. elongatus* on tissue oxygenation, we used a phosphorescent probe to measure oxygen tension at multiple time points after ischemia in an acute myocardial infarction rodent model. Use of a phosphorescent probe (*16*) enabled us to measure tissue oxygenation directly while avoiding off-target scatter from ventricular blood. Briefly, oxygen tension was quantified at baseline and 10 min after left anterior descending (LAD) coronary artery occlusion with initiation of acute ischemia. At this point, animals were randomized to receive direct intramyocardial *S. elongatus* injection in the light, *S. elongatus* injection in the dark, or saline alone. For experiments in the light, injection syringes containing *S. elongatus* were prepared and kept in the incubator under plant lights. For dark experiments, the injection syringes were placed in opaque black bags to prevent light exposure. In the *S. elongatus* (light) and phosphate-buffered saline (PBS) control groups, the hearts were directly exposed to light after injection and for the duration of the experiment. In the *S. elongatus* (dark) groups, injections were performed with dimmed room lights; after injection, room lights were turned off and several layers of aluminum foil were placed over the operative field to shield the heart from light exposure. Tissue oxygen tension was reassessed at 10 and 20 min after injection. We found that baseline oxygen levels were similar among all three groups at 30 torr and predictably dropped to near zero in the ischemic myocardium

(Fig. 2A). In the light, *S. elongatus*–treated hearts demonstrated a nearly 25-fold increase in oxygenation levels from the nadir of ischemia at both 10 and 20 min after *S. elongatus* injection (Fig. 2B). By comparison, both the hearts treated with *S. elongatus* in the dark and the saline-treated group showed only a threefold increase in oxygen tension, likely secondary to diffusion of atmospheric oxygen through the open-chest incision. The finding of elevated tissue oxygenation is critical because it forms the basis for enhanced myocardial bioenergetics (table S1).

Cyanobacterial therapy augments tissue metabolism during acute ischemia

We next turned our attention to evaluating the myocardial metabolic state in vivo. This was accomplished using FLIR thermal imaging videography, an effective method for quantifying in vivo metabolic activity (*17*). Between the light exposed control and *S. elongatus* groups, no difference in baseline left ventricular (LV) surface temperature was observed, with both groups demonstrating a similar relative decrease in temperature, as a ratio to baseline, in the ischemic region after LAD ligation. At 10 min after injection, no significant difference between groups remained; however, at 20 min, the *S. elongatus*–treated group demonstrated a significantly enhanced preservation of surface temperature in the ischemic region (Fig. 2C). Representative thermal images at these four time points are provided (Fig. 2D). The control group showed a steady decrease in ischemic region surface temperature over time, whereas the *S. elongatus* group demonstrated an increase in local temperature from the time of ligation, indicating enhanced metabolic activity (table S2).

S. elongatus therapy enhances ventricular function during acute ischemia

We explored the immediate functional effects of cyanobacterial therapy to determine whether enhanced tissue oxygenation and an up-regulated myocardial metabolic state would improve cardiac mechanics. This was performed using an ascending aortic flow probe for CO quantification and an LV pressure-volume catheter for hemodynamic assessment at baseline after ischemia induction and 45 min after photosynthetic therapy. There was no baseline difference between control and *S. elongatus*–treated groups with regard to the maximum LV pressure (P_{max}), dP/dt, and CO. However, at 45 min after intervention, the *S. elongatus*–treated animals demonstrated augmented P_{max}, dP/dt, and CO (Fig. 2, E to G), consistent with enhanced ventricular contractility and overall cardiac performance (table S3). On average, *S. elongatus* therapy in light resulted in a nearly 30% increase in CO relative to *S. elongatus* therapy in the dark and a nearly 60% increase in CO relative to the ischemic control. To further test our hypothesis that only actively photosynthesizing cyanobacteria provide benefits, we also measured CO in animals that underwent coronary ligation but received *S. elongatus* injections in the dark. In this group, there was no significant increase in CO after injection, supporting our hypothesis (Fig. 2G and table S4). We also tested whether *S. elongatus* has any intrinsic effect on myocardial tissue by injecting animals that did not undergo coronary ligation and monitoring CO. No significant changes in CO from baseline were noted, signifying that *S. elongatus* does not exert intrinsic inotropic or chronotropic effects on the myocardium (Fig. 2G and table S4).

S. elongatus therapy yields durable improvements in ventricular performance after transient ischemia

After establishing the heart's increased bioenergetic and functional state immediately after photosynthetic *S. elongatus* administration during acute ischemia, we next examined the long-term effects of this therapy. To do this, we used an ischemia-reperfusion (IR) rodent model of cardiomyopathy. Briefly, Wistar rats underwent a left thoracotomy to expose the heart and enable consistent light exposure. The animals were randomly selected for sham surgery or myocardial ischemia. In the myocardial ischemia group, the LAD was temporarily occluded to induce ischemia, and animals were randomized to receive injection with saline alone or *S. elongatus*. After 60 min, the occlusion was removed to allow for reperfusion of the ventricle over an additional 60 min while exposed to light before chest closure. Animals were recovered and evaluated over a 4-week time frame. Biochemical analysis at 24 hours after recovery revealed that serum troponin, a clinical marker of myocardial injury and infarction, was significantly reduced in the *S. elongatus*–treated group (Fig. 3A). This finding suggests a long-term myocardial protective effect from photosynthesis-driven bioenergetics.

Cardiac magnetic resonance imaging (MRI) analysis at the 4-week time point revealed a significantly augmented LV ejection fraction and reduced end-systolic volume in *S. elongatus*–treated animals (Fig. 3, B to E), consistent with improved cardiac function and mitigated pathologic remodeling. Further supporting this finding, intraventricular catheterization demonstrated significantly improved LV contractility as determined by the end-systolic pressure-volume relationship (Fig. 3, F to H). Overall, these findings strongly support a long-term protective benefit of photosynthetic therapy, which translates to enhanced cardiac performance (table S5).

Cyanobacterial therapy is nontoxic and nonpathogenic

After demonstration of the benefits of cyanobacterial therapy, we evaluated the potential in vivo toxicity and immune response to the injected microbes. Animals were randomized to receive an intravenous injection of 1-ml saline control or 5×10^8 *S. elongatus*. Blood samples were then acquired at multiple time points over a 1-week period to assess for infection and immune response. Clinically, the animals demonstrated no signs of infection. Blood cultures were also persistently negative for bacterial growth over the study period. Serial flow cytometry of serum indicated no difference in CD8 T cell and CD19 B cell populations (Fig. 4A). There was also no difference in the circulating CD4 population (Fig. 4B).

Along with evaluating the systemic immune response in animals receiving intravenous *S. elongatus*, we carried out immunohistochemistry and histological analyses of cardiac tissue at various times after injection to ascertain the local effects of *S. elongatus* injection. Immunohistochemistry of tissue from the acute ischemia model, taken approximately 1 hour after injection, demonstrated a substantial tissue burden of *S. elongatus* (Fig. 4C). By 24 hours after injection, nearly all injected cyanobacteria had been cleared, with only a small number of cells remaining in the interstitium (Fig. 4D). There was no obvious immune reaction at the 1- and 24-hour time points, and stains for major histocompatibility complex (MHC) class II were negative. Animals from the IR model were used to determine long-term local effects of *S. elongatus* injection. After euthanasia of animals from the 4-week IR experiments, the hearts were explanted to assess abscess formation and the presence of retained *S. elongatus*. Hematoxylin and eosin staining, as well as immunohistochemistry, showed no evidence of either abscess formation or residual *S. elongatus* at 4 weeks after therapy (Fig. 4, E to H). These data suggest that *S. elongatus* therapy is nontoxic and does not elicit a meaningful pathologic immune response.

DISCUSSION

This study demonstrates the first successful utilization of a photosynthetic system as a means of correcting tissue ischemia. The *S. elongatus*

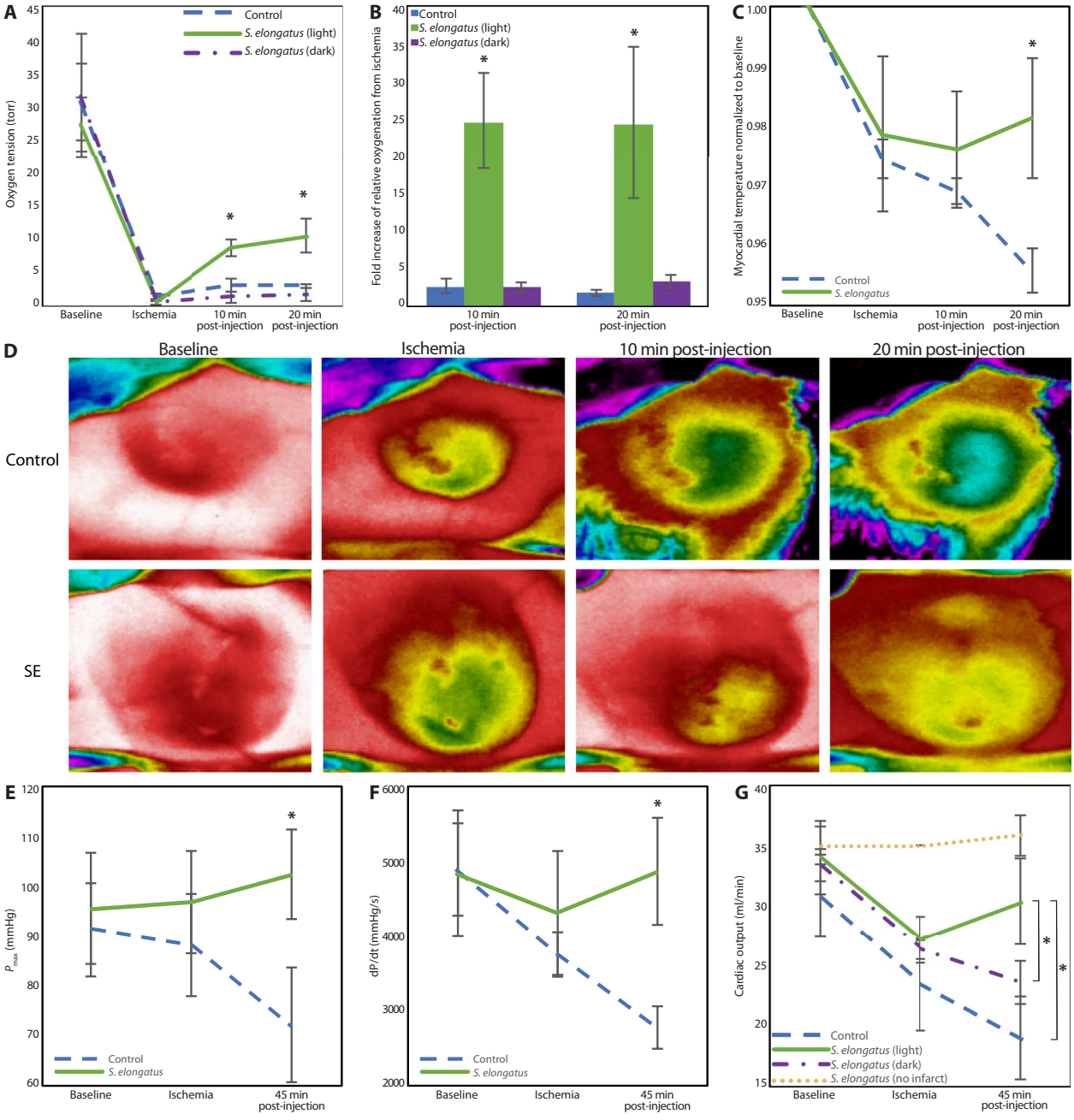

Fig. 2. Enhancement of oxygenation, metabolism, and cardiac function in acute ischemia. Animals were randomized to receive saline control ($n = 5$), *S. elongatus* therapy in light ($n = 5$), and *S. elongatus* therapy in dark ($n = 5$). (**A**) Phosphorescent probe technology was used to quantify tissue oxygenation at baseline, time of ischemia, and 10 and 20 min after therapy. Oxygen tension was significantly higher in the *S. elongatus* (light)–treated group compared with controls and *S. elongatus* (dark) groups at 10 (group-time interaction, $P = 0.004$) and 20 (group-time interaction, $P = 0.003$) min after injection. (**B**) Compared with the control and *S. elongatus* (dark) groups, the *S. elongatus* (light)–treated group showed significantly elevated levels of tissue oxygenation at 10 ($P = 0.002$) and 20 ($P = 0.004$) min after injection with an almost 25-fold increase relative to the time of ischemia. (**C**) Thermal imaging was used to quantify epicardial surface temperature as a measure of myocardial energetics. *S. elongatus*–treated animals demonstrated significantly increased surface temperature at 20 min after therapy ($P = 0.04$) with a positive trajectory. (**D**) Representative thermal images. (**E** and **F**) Pressure-volume assessment revealed significantly enhanced maximum LV pressure (E) ($P = 0.04$) and dP/dt (F) ($P = 0.02$) at 45 min after therapy. (**G**) An ascending aortic flow probe was used to measure CO. At 45 min after therapy, CO in the *S. elongatus* (light) group was significantly higher than the control group and *S. elongatus* (dark) group (group-time interaction, $P = 0.05$). All data are reported as means ± SEM. *$P < 0.05$ using a repeated-measures analysis of variance (ANOVA) for (A), (B), and (G) and two-tailed unpaired Student's t test for (C), (E), and (F).

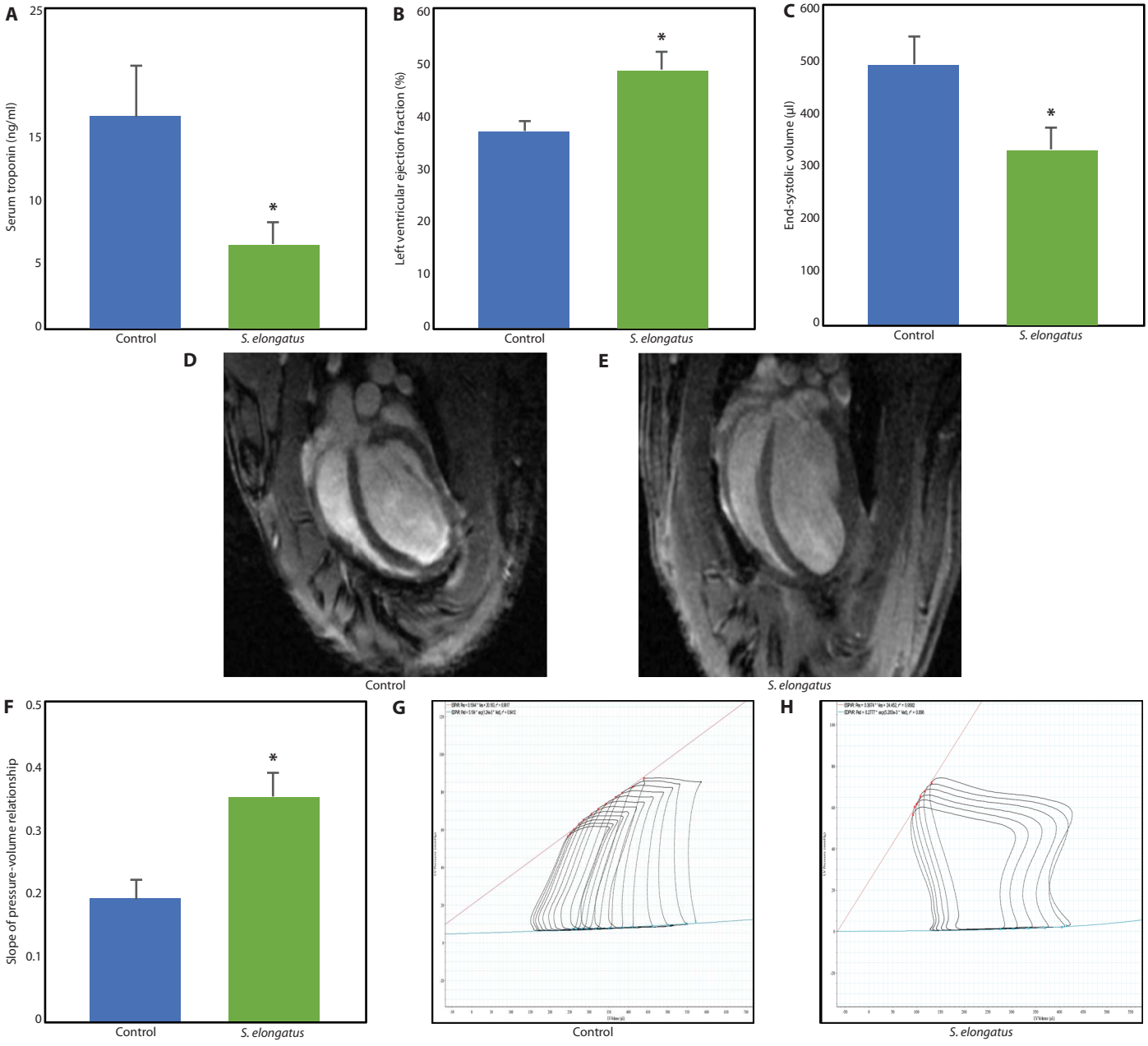

Fig. 3. Long-term protective and functional benefit of photosynthetic therapy. Animals underwent myocardial IR injury and were randomized to saline control ($n = 7$), *S. elongatus* therapy ($n = 10$), or sham surgery ($n = 7$). (**A**) Serum troponin at 24 hours after injury was substantially reduced in the *S. elongatus* group compared with saline controls ($P = 0.05$), indicating ameliorated myocardial injury. (**B**) LV ejection fraction was increased in the *S. elongatus* group ($P = 0.02$) determined by cardiac MRI. (**C**) End-systolic volume was decreased in the *S. elongatus*–treated animals ($P = 0.03$), illustrating reduced pathologic remodeling. (**D** and **E**) Representative four-chamber cardiac MRI images. (**F** to **H**) *S. elongatus* therapy resulted in a greater slope of the LV pressure-volume relationship during inferior vena cava occlusion ($P = 0.01$), indicating enhanced ventricular contractility. All data reported as means ± SEM. *$P < 0.05$ using two-tailed unpaired Student's *t* test.

use interstitial H_2O and CO_2 released by the oxygen-depleted cell and convert it to glucose and O_2 with light serving as the energy source. Glucose produced by *S. elongatus* is retained by the cyanobacterium themselves and likely does not benefit ischemic cardiomyocytes; however, oxygen levels are significantly increased. By helping balance a pathologically unbalanced equation, cardiomyocytes are protected, translating to improved cardiac function. The data show that *S. elongatus* can be efficiently used, allowing for direct delivery to ischemic myocardium. This treatment resulted in augmented tissue oxygenation, increased myocardial surface temperature likely secondary to metabolic activity, and greatly enhanced LV function in an ischemic setting. Although the absolute increase in CO in *S. elongatus* (light) injections compared to the *S. elongatus* (dark) injections seems relatively small and is somewhat variable, on average, it resulted in a nearly 30% increase in CO. In humans, an increase of this magnitude would have profound clinical implications, likely representing the difference between a healthy patient and one suffering from heart failure. Immunologic analysis demonstrated no obvious inflammatory response to the therapy. After intravenous delivery

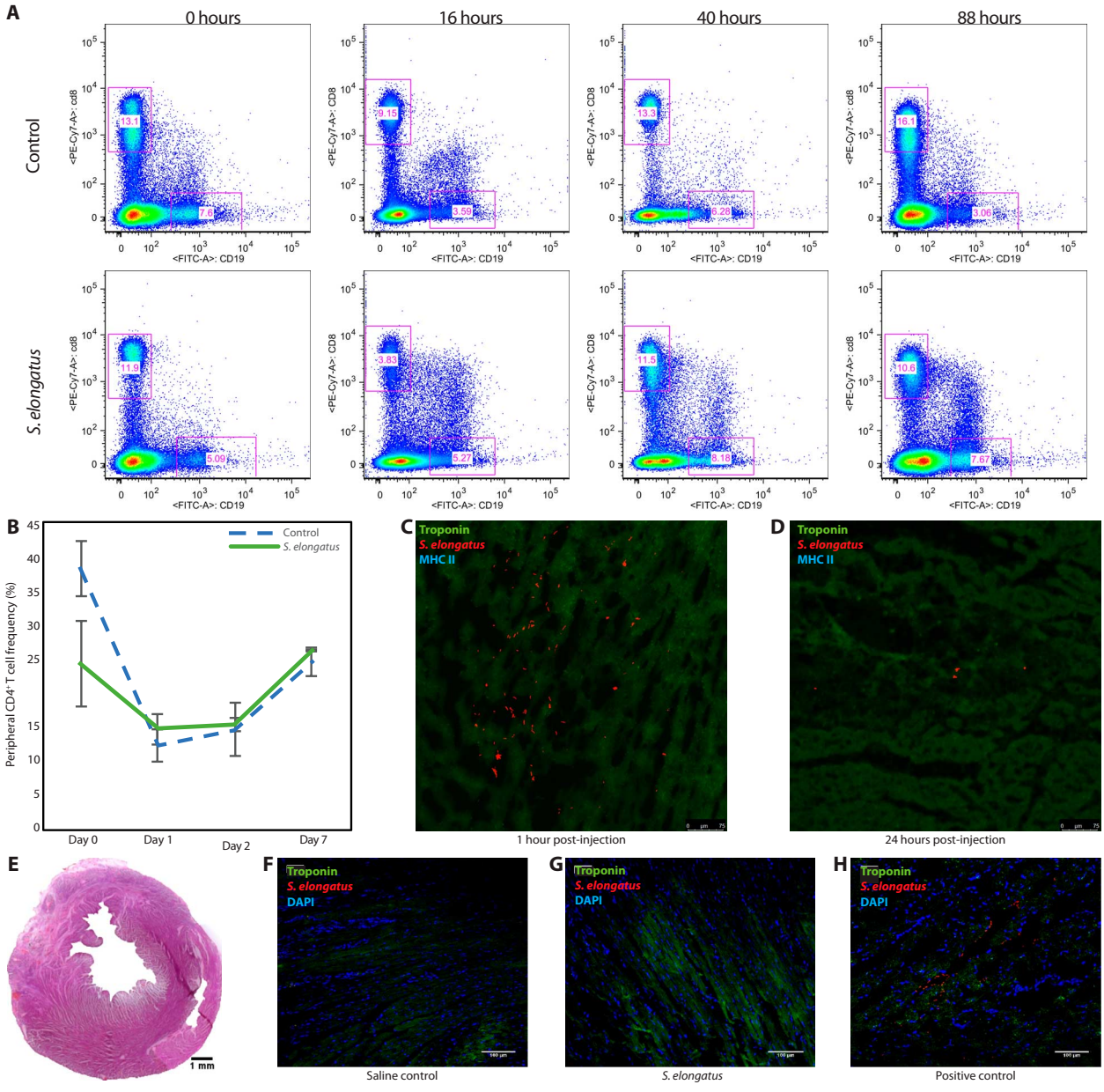

Fig. 4. *S. elongatus* therapy does not elicit a pathologic immune response nor persist in tissue long-term. (**A**) Flow cytometry of blood at 0, 16, 40, and 88 hours after intravenous administration of saline ($n = 4$) or *S. elongatus* ($n = 4$), demonstrating no difference in $CD8^+$ T cell and $CD19^+$ B cell frequencies. PE, phycoerythrin; FITC, fluorescein isothiocyanate. (**B**) No differences in peripheral $CD4^+$ T cell frequencies at 0, 1, 2, and 7 days were observed (means ± SD). (**C** and **D**) Immunohistochemistry of heart sections at 1 hour after injection (C) and 24 hours after injection (D), demonstrating marked reduction of *S. elongatus* present in the tissue. (**E**) Representative hematoxylin and eosin–stained heart section revealing no abscess at 4 weeks after therapy. (**F** and **G**) Immunohistochemistry of heart sections at 4 weeks, illustrating no evidence of retained *S. elongatus*. All data reported as means ± SEM. DAPI, 4′,6-diamidino-2-phenylindole.

of 5×10^8 *S. elongatus* cells, blood cultures remained negative and the animals showed no clinical signs of infection for the duration of the 1-week observation period. The persistence of *S. elongatus* in the tissue is likely short-lived, with most of the injected cells cleared from the tissue by 24 hours. As such, this proposed therapy holds most potential in situations where a temporary supply of oxygen is required, such as during acute myocardial infarction before revascularization.

As briefly mentioned, increased tissue oxygenation forms the basis for enhanced myocardial bioenergetics. By allowing aerobic respiration to occur, adenosine triphosphate production is greatly enhanced, whereas lactic acid release is mitigated with the decrease in anaerobic glycolysis. Clinically, this principle is used universally as providers strive to revascularize ischemic myocardium as quickly as possible in the setting of a myocardial infarction (*18*). In this model, by quickly restoring oxygenation after an acute LAD occlusion, the heart demonstrated increased metabolic activity and improved ventricular function. Using *S. elongatus* to mitigate acute tissue ischemia has a range of possibilities, including its use as an adjunctive cardioplegia during cardiopulmonary bypass surgery or as a transplant organ perfusate to provide tissue with oxygen in the absence of blood flow during transport.

In addition to restoring oxygenation during ischemia, *S. elongatus* therapy may also exert beneficial effects after the restoration of blood flow. It has been demonstrated that, even after revascularization with coronary artery bypass grafting or percutaneous coronary intervention, a significant residual microvascular perfusion deficit remains (*19*, *20*). This leads to progressive ventricular remodeling (*21*), ischemic cardiomyopathy, heart failure, and death (*22*), which many survivors of acute myocardial infarction will eventually succumb to. Angiogenic cytokine and stem cell–based therapies have been studied to address these issues; however, these treatments can take days to weeks to induce a substantial therapeutic response, potentially limiting the amount of myocardium that can be salvaged. *S. elongatus*, either alone or as an adjunct to cell or cytokine therapies, may be an effective means of addressing microvascular disease and mitigating the development of the late ischemic cardiomyopathy.

Our IR experiments support the fact that this strategy may be effective and translatable. We demonstrated that 2 hours of active therapy while the heart was exposed to light resulted in significant functional benefits and preserved ventricular architecture 4 weeks later. These benefits are presumably due to increased tissue oxygenation during the period of hypoxia, allowing a greater number of cells to survive until blood flow is restored. Although it is possible that the cyanobacteria alleviate microvascular perfusion deficits after reperfusion, resulting in additional benefits, it is not possible to quantify this with certainty; this is a limitation of our study. Despite these limitations, the observed benefits do have significant clinical implications, indicating that *S. elongatus* therapy could be used as an immediate adjunct to current medical interventions for patients suffering an acute myocardial infarction. A limiting factor to this particular application is the need for the tissue to be in direct light, necessitating an open incision for the delivery of photons, because most cases of acute myocardial infarction are treated in the cardiac catheterization suite. However, recently, a new chlorophyll pigment, chlorophyll f, that absorbs light in the infrared spectrum, was identified in other cyanobacteria (*23*); using a strain of cyanobacteria active in the far-red spectrum could potentially allow for transcutaneous delivery of energy. Combining transcutaneous energy delivery with percutaneous or intracoronary administration of *S. elongatus* would be a promising step toward human translation. Genetically engineering *S. elongatus* to actively export glucose has been described. *S. elongatus* produces intracellular sucrose to balance osmolarity in its saltwater environment; this feature can be exploited to create a strain of *S. elongatus* that produces and exports high levels of carbohydrates (*24*). By using homologous recombination, the *Zymomonas mobiles invA* gene that codes for invertase can be introduced, which allows intracellular sucrose to be cleaved into fructose and glucose before being actively extracellularly exported along with the *glf* gene encoding a glucose/fructose-facilitated diffusion transporter (*15*). Extracellular sodium chloride concentration can then be manipulated to adjust the amount of glucose produced. We have preliminarily explored this technique, creating a plasmid containing these genes and creating an enhanced glucose producing strain of *S. elongatus* through transformation with some early success. This avenue of research could substantially improve the efficacy of cyanobacterial therapy and bring the technology closer to clinical translation.

Although extremely different from any known strategy addressing myocardial ischemia, the use of *S. elongatus* to provide ischemic cardiomyocytes with oxygen via photosynthesis represents a novel and potentially feasible approach to treating the ischemic heart. Because *S. elongatus* is amenable to genetic engineering (*25*), there are countless possibilities regarding the augmentation of energy production, in vivo tracking, and growth control. Although obstacles exist, as with any new therapy in its infancy, the data suggest a very real benefit from the use of photosynthesis to treat ischemic disease. In addition, the ability to treat ischemic tissue without the need for blood flow has far-reaching implications beyond just the ischemic heart. Thus, the next stage of developing this photosynthetic strategy will focus on elucidating and proving the exact mechanisms coupled with enhancing clinical translatability with biomedical engineering.

MATERIALS AND METHODS

Propagation of *S. elongatus*

One frozen *S. elongatus* vial (catalog no. A14259, Life Technologies Corporation) was transferred from the −80°C freezer onto dry ice. Thirty milliliters of room temperature Gibson BG-11 medium (catalog no. A1379902, Life Technologies) was added to one baffled bottom flask with vented cap (catalog no. 4116-0125, Thermo Fisher Scientific Inc.). Cells were quickly thawed in a 35°C water bath without agitating the vial. The full content was transferred into a flask containing culture medium. The culture was placed on a rotating incubator (model no. 420, Thermo Electron Corporatio) running at 34°C and 125 rpm. A lamp with two 18-inch plant fluorescent light bulbs (F18T8 PL/AQ, General Electric) was placed on the incubator to allow light to reach the culture. Initial outgrowth of the culture took 5 to 7 days. The culture was maintained by adding fresh BG-11 medium daily to replace evaporative losses and maintain a constant volume. Every 4 days, or whenever the colony becomes noticeably oversaturated, as indicated by clumping or sediment collecting at the bottom of the flask, approximately 25% of the colony was discarded and replaced with an equal volume of fresh BG-11.

In vitro experimental model

Cardiomyocytes were isolated from 1- to 3-day-old neonatal rats using an isolation kit (Pierce Primary Cardiomyocyte Isolation Kit, Thermo Fisher Scientific Inc.) according to the manufacturer's instructions. On 24-well tissue culture plates, three wells were plated with isolated cardiomyocytes at a density of 500,000 cells per well, three wells were plated with the same density of cardiomyocytes along 10^7 *S. elongatus*, three wells contained 10^7 *S. elongatus* alone, and three wells contained cell growth medium alone. Dulbecco's modified Eagle's medium with 10% FBS was used as the growth medium for all wells. The plates were cultured at 37°C for 16 hours under various conditions depending on the experiment. For experiments comparing the effect of *S. elongatus* in light and dark conditions the above-mentioned 18-inch fluorescent plant bulbs were used as the light source; dark samples were placed in opaque black bags to prevent light exposure. For experiments requiring hypoxia, we created a hypoxic environment using vacuum-sealed bags and a hypoxic gas mixture containing 1% oxygen, 5% carbon dioxide, and nitrogen balance (Praxair Inc.). The bags were flushed with hypoxic gas for approximately 5 min to ensure that all atmospheric air was expelled before being heat-sealed. In vitro oxygen measurements were obtained as described below. To assess cellular viability, a live/dead viability/cytotoxicity assay (catalog no. L3224, Thermo Fisher Scientific Inc.) was performed and analyzed using fluorescent microscopy (Leica DMi8, Leica). Briefly, red fluorescent ethidium homodimer-1 was used to stain the nuclei of dead cells (those without intact plasma membranes), and green fluorescent calcein-acetoxymethyl was used to mark intracellular esterase activity of living cells. Dead cells were visible as small red spheres, whereas the cytoplasm of living cells was green. *S. elongatus* autofluorescenced at the same wavelength as the emission wavelength of the red

fluorescent dye that bound to dead animal cells and showed up as thin red rods. The Fiji distribution of ImageJ and built-in Cell Counter plugin were used to count the number of live and dead cells (*26*). The live/dead experiments were performed in triplicate, and three images were obtained for each well. A grid was first created on each image using ImageJ; next, the Cell Counter plugin was used to mark and count the number of live and dead cells. The total cell count was calculated by adding the number of live cells to the number of dead cells, which was averaged before statistical analysis. To measure cellular metabolism, a WST-1 cell proliferation assay (catalog no. ab155902, Abcam plc.) was performed and analyzed on a plate reader (Synergy 2, BioTek). For experiments requiring the measurement of glucose, a sucrose/fructose/D-glucose assay was used (K-SUFRG, Megazyme International Ltd. Bray Co.) according to the manufacturer's instructions. Electron microscopy was performed on a field emission scanning electron microscope (Zeiss Sigma FESEM, Carl Zeiss AG) with the following settings: electronic high tension, 2.00 kV; working distance, 5.2 mm; signal A, InLens; and magnification, 5.73 KX (fig. S1). A raster graphics editor (Adobe Photoshop CC 2015.5, Adobe Systems) was used to create a false-colored scanning electron micrograph (fig. S2).

In vitro oxygen tension measurements

Phosphorescence lifetime measurements were used to measure in vitro oxygen tension using a NEOFOX-GT optical oxygen sensor with a phosphor coating baked onto the glass fiber (Ocean Optics). The probe was calibrated using nitrogen bubbled through water for the 0% reading, and water was equilibrated with the atmosphere for the 20.9% reading. The integrated software included with the system was used to interpret the optical signal, convert to torr, and acquire data. Temperature correction was achieved with a thermistor probe.

Rat model of acute myocardial ischemia and IR

For both the acute myocardial ischemia and IR models, male Wistar rats (300 to 350 g) were sedated in an isoflurane chamber, intubated with a 16-gauge angiocatheter, and mechanically ventilated (Hallowell) on 2.0% isoflurane maintenance.

In the acute myocardial infarction model, the right carotid artery was dissected free, and an SPR-869 pressure-volume catheter (Millar) was introduced into the left ventricle via the carotid. A median sternotomy was then performed, and the ascending aorta was dissected free for placement of a flow probe (Transonic) to continuously monitor CO (fig. S3). Baseline hemodynamics were then acquired. To induce myocardial ischemia, we permanently occluded the LAD with a 6-0 polypropylene suture 2 mm below the level of the left atrial appendage. After 15 min, hemodynamic data were collected, and animals were randomized ($n = 5$ per group) to receive intramyocardial injections of either PBS or 1×10^6 *S. elongatus* suspended in PBS directly to the ischemic territory. We prepared the *S. elongatus* injections first by determining the concentration of the culture. The proper number of cyanobacteria was then collected by centrifugation, the medium was aspirated, and dilutions were prepared by resuspending the cells in the proper volume of PBS to obtain a concentration of 1×10^6 cells in 100 µl. For injections performed in the light, injection syringes were kept in the incubator under plant lights after preparation but before injection (approximately 2 hours). After injection, the heart and surrounding tissues were directly exposed to light for the remainder of the acute experiments and until chest closure in the IR experiments. For injections in the dark, after the injection syringes were prepared, they were placed in black opaque bags, shielding them from light inside the incubator. During injection, room lights were turned off, and only the minimum amount of indirect light needed by the surgeon to see the operative field was used. After injection, lights were turned off completely, and the operative field was covered with several layers of aluminum foil to shield the tissue from inadvertent light exposure for the remainder of the acute experiments and until chest closure in the IR model. In the IR model, chest closure was performed with only the minimum amount of indirect light needed by the surgeon to see the operative field. For intramyocardial injections, we used a 31-gauge insulin syringe with the needle bent slightly to enter parallel to the endocardium. Before injection, we drew back slightly on the plunger of the syringe to ensure that the needle was not intraventricular; we visually checked for wheal formation as we injected for further confirmation that the injection was intramyocardial. Both groups were exposed to high-intensity direct light through the open-chest incision. Hemodynamics were then serially acquired every 15 min for 45 min until the animals were euthanized at 45 min. In addition, intramyocardial oxygen tension and thermal imaging was acquired at baseline, at time of ischemia, and at 10 and 20 min after injection, as described in further detail below. After the initial acute experiments, additional control groups were included in the analysis, including injecting *S. elongatus* under dark conditions in animals after coronary ligation ($n = 5$), as well as injecting *S. elongatus* in animals that did not undergo coronary ligation ($n = 5$). Intramyocardial oxygen tension and CO were acquired as described above.

For the IR model, a left thoracotomy was used. Animals were randomized to receive sham surgery ($n = 7$) or myocardial ischemia ($n = 17$). The LAD was temporarily occluded with a 6-0 polypropylene suture, which was passed through a segment of small plastic tube and then clamped with a hemostat to fashion a tourniquet. Animals were then randomized to receive injection with PBS control ($n = 7$) or 1×10^6 *S. elongatus* suspended in PBS ($n = 10$). After 60 min under direct light condition, the tourniquet was removed from the LAD and reperfusion with an open chest under direct light was allowed to occur for an additional 60 min before closing the chest and recovering the animal. Serum was collected at 24 hours to assess for troponin level. At 4 weeks, animals underwent cardiac MRI. Imaging was performed using a 7-T VNMRS horizontal bore scanner (Varian Inc.) with a shielded gradient system (400 mT/m). Both two- and four-chamber cines were acquired. Functional and architectural analysis was performed in a blinded fashion. After cardiac MRI, animals underwent LV catheterization for hemodynamic assessment as described, followed by euthanasia. Baseline LV pressure-volume loops were unable to be obtained because LV catheterization is a terminal procedure in rats. After euthanasia, the hearts were explanted for immunohistochemistry and histological analysis, as described in further detail below.

Intramyocardial oxygen tension acquisition

Phosphorescence lifetime measurements were performed using a PMOD-5000 phosphorometer (Oxygen Enterprises). The PMOD-5000 is a frequency domain instrument operating in the range of 100 to 100,000 Hz. The measured phosphorescence lifetimes were independent of local phosphor concentration and insensitive to the presence of endogenous tissue fluorophores and chromophores. The excitation light was transmitted to the measurement site through a glass fiber bundle, and the emission was collected by another 3-mm-diameter glass fiber bundle (center-to-center distance of 6 mm). The emission was passed through a 695-nm long-pass glass filter (Schott glass) and detected by an avalanche photodiode (Hamamatsu). The resulting photocurrent was

converted into voltage, amplified, digitized, and transferred to a computer for analysis. Data were acquired at baseline, at time of ischemia, and at 10 and 20 min after injection.

Thermal imaging

For thermal imaging to assess surface myocardial heat emission and examine metabolic activity, FLIR A655sc camera was used. Care was taken to maintain a constant body temperature with a heating pad. In addition, the camera was precisely placed and mechanically stabilized 30 cm above the chest. At 20 min after cyanobacteria injection, thermal images were acquired and then analyzed with FLIR software to determine myocardial surface temperature.

Immunological analysis and flow cytometry

Male Wistar rats were sedated and intravenously administered with either saline ($n = 4$) or 5×10^8 cyanobacteria ($n = 4$). Before administration, blood samples were acquired for flow cytometry to examine inflammatory markers. At 16 hours after administration, blood was acquired for culture and flow cytometry. This was repeated at 40 and 88 hours. Blood cultures were performed at the Stanford Animal Diagnostic Laboratory. Flow cytometry was performed by placing 100 µl of peripheral blood into BD Microcontainer tubes with dipotassium EDTA. Blood was transferred into 5-ml polystyrene Falcon tubes with 4-ml ammonium chloride and Na acetate buffer and remained on ice for 10 min. The red blood cell lysis was repeated a second time. The pellet was rinsed in PBS + 2% FBS, and cells were stained for membrane proteins (CD19, CD8, CD11b, and Ly-6G) for 1 hour in a 4°C cold room. Cells were resuspended in 200 µl of PBS, and flow cytometry analysis was carried out on BD Biosciences LSR II at the Stanford Shared FACS Facility.

Immunohistochemistry and histology

Immunohistochemistry and histology samples were taken at various time points after injection. In animals from the acute experiments, euthanasia was performed with potassium chloride after data collection approximately 1 hour after injection, and the hearts were explanted and prepared, as described below. In animals from the IR experiment, at 4 weeks' posttherapy after euthanasia, the hearts were explanted for analysis. Whole-heart specimens were immediately flushed with PBS, injected retrograde with Tissue-Tek optimum cutting temperature (OCT) (Sakura) through the aorta and pulmonary artery, submerged in OCT., frozen at −80°C, and sectioned onto glass slides using a Leica CM3050S cryostat (Leica) at a thickness of 10 µm. Next, the samples were fixed with 4% paraformaldehyde and blocked with 10% FBS. For immunohistochemistry of acute and 24-hour injection specimens, sections were stained with cardiac troponin primary antibody at 1:200 dilution (ab39807, Abcam) with Alexa Fluor 405 secondary antibody at 1:200 dilution (ab175664, Abcam), and MHC class II primary antibody at 1:200 dilution (ab116378, Abcam) with Alexa Fluor 488 secondary antibody (ab150065, Abcam) at 1:200 dilution. For immunohistochemistry of IR specimens, sections were stained with cardiac troponin primary antibody at 1:200 dilution (ab47003, Abcam) and a fluorescein isothiocyanate secondary antibody (ab6717, Abcam) at a 1:200 dilution and counterstained with 4′,6-diamidino-2-phenylindole (Vector Laboratories). The sections were imaged with a Leica DM5000B fluorescent microscope and a Leica DMi8 fluorescent microscope. The *S. elongatus* were fluorescent at the 596-nm red channel of the scope. For histological analysis, sections were stained with hematoxylin and eosin for assessment of abscess presence.

Animal care

All experiments pertaining to this investigation conformed to the *Guide for the Care and Use of Laboratory Animals*, published by the U.S. National Institutes of Health (eighth edition, 2011) under the supervision of the Stanford Administrative Panel on Laboratory Animal Care, Stanford's Institutional Animal Care and Use Committee, which is accredited by the Association for the Assessment and Accreditation of Laboratory Animal Care.

Statistical analysis

All analyzed variables approximated a normal distribution. Values for continuous variables were reported as means ± SD. Two-tailed unpaired Student's *t* tests were used to compare continuous variables between two groups. Repeated-measures ANOVA was used to compare continuous variables between groups across multiple time points. A P value of <0.05 was considered statistically significant.

SUPPLEMENTARY MATERIALS

Supplementary material for this article is available at http://advances.sciencemag.org/cgi/content/full/3/6/e1603078/DC1

fig. S1. High-resolution grayscale scanning electron micrograph before false coloring.
fig. S2. High-resolution false-colored scanning electron micrograph.
fig. S3. In vivo rodent model of acute myocardial infarction.
table S1. Effect of *S. elongatus* therapy on myocardial oxygenation in acute ischemia model.
table S2. Effect of *S. elongatus* therapy on myocardial surface temperature in acute ischemia model.
table S3. Effect of *S. elongatus* therapy on LV hemodynamics in acute ischemia model.
table S4. Effect of *S. elongatus* therapy on CO in acute ischemia model.
table S5. Long-term effect of *S. elongatus* therapy on LV function in IR model.

REFERENCES AND NOTES

1. D. Mozaffarian, E. J. Benjamin, A. S. Go, D. K. Arnett, M. J. Blaha, M. Cushman, S. de Ferranti, J.-P. Després, H. J. Fullerton, V. J. Howard, M. D. Huffman, S. E. Judd, B. M. Kissela, D. T. Lackland, J. H. Lichtman, L. D. Lisabeth, S. Liu, R. H. Mackey, D. B. Matchar, D. K. McGuire, E. R. Mohler, C. S. Moy, P. Muntner, M. E. Mussolino, K. Nasir, R. W. Neumar, G. Nichol, L. Palaniappan, D. K. Pandey, M. J. Reeves, C. J. Rodriguez, P. D. Sorlie, J. Stein, A. Towfighi, T. N. Turan, S. S. Virani, J. Z. Willey, D. Woo, R. W. Yeh, M. B. Turner; American Heart Association Statistics Committee and Stroke Statistics Subcommittee, Heart disease and stroke statistics—2015 update: A report from the American Heart Association. *Circulation* **131**, e29–e322 (2015).
2. Y. Tian, Y. Liu, T. Wang, N. Zhou, J. Kong, L. Chen, M. Snitow, M. Morley, D. Li, N. Petrenko, S. Zhou, M. Lu, E. Gao, W. J. Koch, K. M. Stewart, E. E. Morrisey, A microRNA-Hippo pathway that promotes cardiomyocyte proliferation and cardiac regeneration in mice. *Sci. Transl. Med.* **7**, 279ra38 (2015).
3. B. D. Polizzotti, B. Ganapathy, S. Walsh, S. Choudhury, N. Ammanamanchi, D. G. Bennett, C. G. dos Remedios, B. J. Haubner, J. M. Penninger, B. Kühn, Neuregulin stimulation of cardiomyocyte regeneration in mice and human myocardium reveals a therapeutic window. *Sci. Transl. Med.* **7**, 281ra45 (2015).
4. I. J. Fox, G. Q. Daley, S. A. Goldman, J. Huard, T. J. Kamp, M. Trucco, Use of differentiated pluripotent stem cells in replacement therapy for treating disease. *Science* **345**, 1247391 (2014).
5. Y.-D. Lin, C.-Y. Luo, Y.-N. Hu, M.-L. Yeh, Y.-C. Hsueh, M.-Y. Chang, D.-C. Tsai, J.-N. Wang, M.-J. Tang, E. I. H. Wei, M. L. Springer, P. C. H. Hsieh, Instructive nanofiber scaffolds with VEGF create a microenvironment for arteriogenesis and cardiac repair. *Sci. Transl. Med.* **4**, 146ra109 (2012).
6. J. E. Cohen, B. P. Purcell, J. W. MacArthur, A. Mu, Y. Shudo, J. B. Patel, C. M. Brusalis, A. Trubelja, A. S. Fairman, B. B. Edwards, M. S. Davis, G. Hung, W. Hiesinger, P. Atluri, K. B. Margulies, J. A. Burdick, Y. J. Woo, A bioengineered hydrogel system enables targeted and sustained intramyocardial delivery of neuregulin, activating the cardiomyocyte cell cycle and enhancing ventricular function in a murine model of ischemic cardiomyopathy. *Circ. Heart Fail.* **7**, 619–626 (2014).
7. O. Ishida, I. Hagino, N. Nagaya, T. Shimizu, T. Okano, Y. Sawa, H. Mori, T. Yagihara, Adipose-derived stem cell sheet transplantation therapy in a porcine model of chronic heart failure. *Transl. Res.* **165**, 631–639 (2015).

8. J. W. MacArthur, J. E. Cohen, J. R. McGarvey, Y. Shudo, J. B. Patel, A. Trubelja, A. S. Fairman, B. B. Edwards, G. Hung, W. Hiesinger, A. B. Goldstone, P. Atluri, R. L. Wilensky, J. J. Pilla, J. H. Gorman, R. C. Gorman, Y. J. Woo, Preclinical evaluation of the engineered stem cell chemokine stromal cell–derived factor 1α analog in a translational ovine myocardial infarction model. *Circ. Res.* **114**, 650–659 (2014).
9. D. D. Ascheim, A. C. Gelijns, D. Goldstein, L. A. Moye, N. Smedira, S. Lee, C. T. Klodell, A. Szady, M. K. Parides, N. O. Jeffries, D. Skerrett, D. A. Taylor, J. E. Rame, C. Milano, J. G. Rogers, J. Lynch, T. Dewey, E. Eichhorn, B. Sun, D. Feldman, R. Simari, P. T. O'Gara, W. C. Taddei-Peters, M. A. Miller, Y. Naka, E. Bagiella, E. A. Rose, Y. J. Woo, Mesenchymal precursor cells as adjunctive therapy in recipients of contemporary left ventricular assist devices. *Circulation* **129**, 2287–2296 (2014).
10. A. W. Heldman, D. L. DiFede, J. E. Fishman, J. P. Zambrano, B. H. Trachtenberg, V. Karantalis, M. Mushtaq, A. R. Williams, V. Y. Suncion, I. K. McNiece, E. Ghersin, V. Soto, G. Lopera, R. Miki, H. Willens, R. Hendel, R. Mitrani, P. Pattany, G. Feigenbaum, B. Oskouei, J. Byrnes, M. H. Lowery, J. Sierra, M. V. Pujol, C. Delgado, P. J. Gonzalez, J. E. Rodriguez, L. L. Bagno, D. Rouy, P. Altman, C. W. P. Foo, J. da Silva, E. Anderson, R. Schwarz, A. Mendizabal, J. M. Hare, Transendocardial mesenchymal stem cells and mononuclear bone marrow cells for ischemic cardiomyopathy: The TAC-HFT randomized trial. *JAMA* **311**, 62–73 (2014).
11. V. Karantalis, D. L. DiFede, G. Gerstenblith, S. Pham, J. Symes, J. P. Zambrano, J. Fishman, P. Pattany, I. McNiece, J. Conte, S. Schulman, K. Wu, A. Shah, E. Breton, J. Davis-Sproul, R. Schwarz, G. Feigenbaum, M. Mushtaq, V. Y. Suncion, A. C. Lardo, I. Borrello, A. Mendizabal, T. Z. Karas, J. Byrnes, M. Lowery, A. W. Heldman, J. M. Hare, Autologous mesenchymal stem cells produce concordant improvements in regional function, tissue perfusion, and fibrotic burden when administered to patients undergoing coronary artery bypass grafting: The prospective randomized study of mesenchymal stem cell therapy in patients undergoing cardiac surgery (PROMETHEUS) trial. *Circ. Res.* **114**, 1302–1310 (2014).
12. J. Espinosa, J. S. Boyd, R. Cantos, P. Salinas, S. S. Golden, A. Contreras, Cross-talk and regulatory interactions between the essential response regulator RpaB and cyanobacterial circadian clock output. *Proc. Natl. Acad. Sci. U.S.A.* **112**, 2198–2203 (2015).
13. T. Kondo, T. Mori, N. V. Lebedeva, S. Aoki, M. Ishiura, S. S. Golden, Circadian rhythms in rapidly dividing cyanobacteria. *Science* **275**, 224–227 (1997).
14. P. M. Shih, J. Zarzycki, K. K. Niyogi, C. A. Kerfeld, Introduction of a synthetic CO_2-fixing photorespiratory bypass into a cyanobacterium. *J. Biol. Chem.* **289**, 9493–9500 (2014).
15. H. Niederholtmeyer, B. T. Wolfstädter, D. F. Savage, P. A. Silver, J. C. Way, Engineering cyanobacteria to synthesize and export hydrophilic products. *Appl. Environ. Microbiol.* **76**, 3462–3466 (2010).
16. W. L. Rumsey, J. M. Vanderkooi, D. F. Wilson, Imaging of phosphorescence: A novel method for measuring oxygen distribution in perfused tissue. *Science* **241**, 1649–1651 (1988).
17. J. D. Crane, E. P. Mottillo, T. H. Farncombe, K. M. Morrison, G. R. Steinberg, A standardized infrared imaging technique that specifically detects UCP1-mediated thermogenesis in vivo. *Mol. Metab.* **3**, 490–494 (2014).
18. A. Bagai, G. D. Dangas, G. W. Stone, C. B. Granger, Reperfusion strategies in acute coronary syndromes. *Circ. Res.* **114**, 1918–1928 (2014).
19. E. J. Velazquez, K. L. Lee, M. A. Deja, A. Jain, G. Sopko, A. Marchenko, I. S. Ali, G. Pohost, S. Gradinac, W. T. Abraham, M. Yii, D. Prabhakaran, H. Szwed, P. Ferrazzi, M. C. Petrie, C. M. O'Connor, P. Panchavinnin, L. She, R. O. Bonow, G. R. Rankin, R. H. Jones, J.-L. Rouleau; STITCH Investigators, Coronary-artery bypass surgery in patients with left ventricular dysfunction. *N. Engl. J. Med.* **364**, 1607–1616 (2011).
20. A. Araszkiewicz, S. Grajek, M. Lesiak, M. Prech, M. Pyda, M. Janus, A. Cieslinski, Effect of impaired myocardial reperfusion on left ventricular remodeling in patients with anterior wall acute myocardial infarction treated with primary coronary intervention. *Am. J. Cardiol.* **98**, 725–728 (2006).
21. G. K. Yankey, T. Li, A. Kilic, G. Cheng, A. Satpute, K. Savai, S. Li, S. L. Moainie, D. Prastein, C. DeFillipi, Z. J. Wu, B. P. Griffith, Regional remodeling strain and its association with myocardial apoptosis after myocardial infarction in an ovine model. *J. Thorac. Cardiovasc. Surg.* **135**, 991–998 (2008).
22. L. Bolognese, N. Carrabba, G. Parodi, G. M. Santoro, P. Buonamici, G. Cerisano, D. Antoniucci, Impact of microvascular dysfunction on left ventricular remodeling and long-term clinical outcome after primary coronary angioplasty for acute myocardial infarction. *Circulation* **109**, 1121–1126 (2004).
23. M. Chen, M. Schliep, R. D. Willows, Z.-L. Cai, B. A. Neilan, H. Scheer, A red-shifted chlorophyll. *Science* **329**, 1318–1319 (2010).
24. D. C. Ducat, J. A. Avelar-Rivas, J. C. Way, P. A. Silver, Rerouting carbon flux to enhance photosynthetic productivity. *Appl. Environ. Microbiol.* **78**, 2660–2668 (2012).
25. C. M. Agapakis, H. Niederholtmeyer, R. R. Noche, T. D. Lieberman, S. G. Megason, J. C. Way, P. A. Silver, Towards a synthetic chloroplast. *PLOS ONE* **6**, e18877 (2011).
26. J. Schindelin, I. Arganda-Carreras, E. Frise, V. Kaynig, M. Longair, T. Pietzsch, S. Preibisch, C. Rueden, S. Saalfeld, B. Schmid, J.-Y. Tinevez, D. J. White, V. Hartenstein, K. Eliceiri, P. Tomancak, A. Cardona, Fiji: An open-source platform for biological-image analysis. *Nat. Methods* **9**, 676–682 (2012).

Acknowledgments: We would like to thank S. Vinogradov for help with oxygen probe formulation and F. Daldal for assistance in culturing the cyanobacteria. **Funding:** This work was funded by the NIH (R01HL089315-01 to Y.J.W.) and the American Heart Association (14POST20380744 to A.B.G. and 17POST33410497 to M.J.P.). **Author contributions:** J.E.C. conceptualized the study, performed the experiments, analyzed the data, and wrote the manuscript. A.B.G. performed the experiments, analyzed the data, and revised the manuscript. M.J.P. performed the experiments, analyzed the data, assisted with the in vitro study design, wrote and revised the manuscript and revisions, formatted the figures, and assisted with the MRI analysis. Y.S. performed the cardiac MRI experiments and analyzed the data. A.N.S. performed the experiments and revised the manuscript. B.B.E. assisted with the in vivo experiments, processed the explanted hearts for sectioning, and performed the histological staining. J.B.P. performed the *S. elongatus* propagation, culture, and immunohistochemistry. J.W.M. performed the experiments and revised the manuscript. M.S.H. performed the experiments and assisted with the histological staining. C.E.B. performed the flow cytometry for immunological analysis. K.J.J. collected the in vitro oxygen data, performed the experiments, and assisted with the microscopy. A.D.T. collected the in vitro oxygen data, performed the experiments, and assisted with the microscopy. J.M.F. collected the in vitro oxygen data, performed the experiments, and analyzed the microscopy images. V.N.T. performed the experiments, prepared and stained the tissue, and collected the in vivo hemodynamic data. A.T.B. assisted in maintaining the *S. elongatus* colony and collecting the in vitro oxygen data. L.M.S. assisted with the in vitro experimental design and analysis. A.E. assisted with the tissue preparation and staining. A.S.F. performed the experiments and tissue preparation for staining. W.H. contributed to the experimental design and manuscript composition. T.V.E. prepared the phosphorescent probes and analyzed the oxygen tension data. W.L.P. analyzed the cardiac MRI images. K.J. assisted in performing and analyzing the thermal videography experiments. J.A.S. performed and analyzed the immunological experiments. Y.J.W. assisted in the study conceptualization and manuscript writing. **Competing interests:** A patent application related to the techniques reported in this article has been filed. J.E.C., A.B.G., and Y.J.W. are authors on a U.S. patent application related to this work filed by Stanford (15/136,612; filed 22 April 2016). The other authors declare that they have no competing interests. **Data and materials availability:** All data needed to evaluate the conclusions in the paper are present in the paper and/or the Supplementary Materials. Additional data related to this paper may be requested from J.E.C. jecohen@stanford.edu.

Submitted 5 December 2016
Accepted 25 April 2017
Published 14 June 2017
10.1126/sciadv.1603078

Citation: J. E. Cohen, A. B. Goldstone, M. J. Paulsen, Y. Shudo, A. N. Steele, B. B. Edwards, J. B. Patel, J. W. MacArthur, M. S. Hopkins, C. E. Burnett, K. J. Jaatinen, A. D. Thakore, J. M. Farry, V. N. Truong, A. T. Bourdillon, L. M. Stapleton, A. Eskandari, A. S. Fairman, W. Hiesinger, T. V. Esipova, W. L. Patrick, K. Ji, J. A. Shizuru, Y. J. Woo, An innovative biologic system for photon-powered myocardium in the ischemic heart. *Sci. Adv.* **3**, e1603078 (2017).

Science Advances

An innovative biologic system for photon-powered myocardium in the ischemic heart

Jeffrey E. Cohen, Andrew B. Goldstone, Michael J. Paulsen, Yasuhiro Shudo, Amanda N. Steele, Bryan B. Edwards, Jay B. Patel, John W. MacArthur, Jr., Michael S. Hopkins, Casey E. Burnett, Kevin J. Jaatinen, Akshara D. Thakore, Justin M. Farry, Vi N. Truong, Alexandra T. Bourdillon, Lyndsay M. Stapleton, Anahita Eskandari, Alexander S. Fairman, William Hiesinger, Tatiana V. Esipova, William L. Patrick, Keven Ji, Judith A. Shizuru and Y. Joseph Woo

Sci Adv **3** (6), e1603078.
DOI: 10.1126/sciadv.1603078